

UNCLASSIFIED

AD NUMBER

ADB008724

LIMITATION CHANGES

TO:

Approved for public release; distribution is unlimited.

FROM:

Distribution authorized to U.S. Gov't. agencies only; Test and Evaluation; DEC 1975. Other requests shall be referred to Air Force Weapons Laboratory, LRO, Kirtland AFB, NM 87117.

AUTHORITY

afwl ltr 7 nov 1986

THIS PAGE IS UNCLASSIFIED

AD Boo 8724

AUTHORITY:

REINL etc

7104 86



✓ AFWL-TR-75-158

AFWL-TR-75-158 ✓ 16

AD B008724

## LINEAR BIDIRECTIONAL SOLENOID ACTUATOR

H. W. Schaefgen

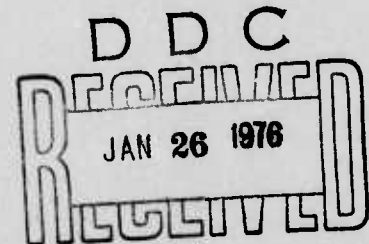
Philco-Ford Corporation  
Aeronutronic Division  
New Port Beach, CA 92663

December 1975

### Final Report

Distribution limited to US Government agencies only because of test and evaluation of military systems (Dec 75). Other requests for this document must be referred to AFWL (LRO), Kirtland AFB, NM 87117

AIR FORCE WEAPONS LABORATORY  
Air Force Systems Command  
Kirtland Air Force Base, NM 87117



AD No. \_\_\_\_\_  
DDC FILE COPY

This final report was prepared by the Philco-Ford Corporation, Aeronutronic Division, New Port Beach, California under Contract F29601-73-C-0060, Job Order 317J0702 with the Air Force Weapons Laboratory, Kirtland Air Force Base, New Mexico. Captain Orest R. Gogosha (LRO) was the Laboratory Project Officer-in-Charge.

When US Government drawings, specifications, or other data are used for any purpose other than a definitely related Government procurement operation, the Government thereby incurs no responsibility nor any obligation whatsoever, and the fact that the Government may have formulated, furnished, or in any way supplied the said drawings, specifications, or other data, is not to be regarded by implication or otherwise, as in any manner licensing the holder or any other person or corporation, or conveying any rights or permission to manufacture, use, or sell any patented invention that may in any way be related thereto.

This technical report has been reviewed and is approved for publication.

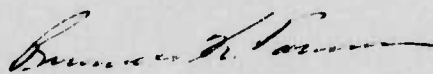


OREST R. GOGOSHA  
Captain, USAF  
Project Officer

FOR THE COMMANDER



BEN F. JOHNSON  
Lt Colonel, USAF  
Chief, Pointing and Tracking Branch



RUSSELL K. PARSONS  
Colonel, USAF  
Chief, Laser Development Division

APPROVED FOR	
DATE	DATE SIGNED <input type="checkbox"/>
BY	DATE SIGNED <input checked="" type="checkbox"/>
UNCLASSIFIED	<input type="checkbox"/>
JUSTIFICATION	
BY	
DISTRIBUTION/AVAILABILITY CODES	
Dist.	AVAIL. and/or SPECIAL
<input checked="" type="checkbox"/>	<input type="checkbox"/>

DO NOT RETURN THIS COPY. RETAIN OR DESTROY.



UNCLASSIFIED

SECURITY CLASSIFICATION OF THIS PAGE (When Data Entered)

19 REPORT DOCUMENTATION PAGE		READ INSTRUCTIONS BEFORE COMPLETING FORM
1. REPORT NUMBER <b>18</b> AFWL-TR-75-158	2. GOVT ACCESSION NO.	3. RECIPIENT'S CATALOG NUMBER
4. TITLE (and Subtitle) <b>6</b> LINEAR BIDIRECTIONAL SOLENOID ACTUATOR.	5. TYPE OF REPORT & PERIOD COVERED <b>9</b> FINAL REPORT,	
7. AUTHOR(s) H. W. SCHAEFGEN <b>10</b> Harold W. Schaeffgen	8. CONTRACT OR GRANT NUMBER(s) <b>15</b> F29601-73-C-0060	
9. PERFORMING ORGANIZATION NAME AND ADDRESS Philco-Ford Corporation Aeronutronic Division New Port Beach, California 92663	10. PROGRAM ELEMENT, PROJECT, TASK AREA & WORK UNIT NUMBERS 63000F, 317J, 07, 02	
11. CONTROLLING OFFICE NAME AND ADDRESS Air Force Weapons Laboratory Kirtland Air Force Base, NM 87117	12. REPORT DATE <b>11</b> December 1975	
13. MONITORING AGENCY NAME & ADDRESS (if different from Controlling Office) <b>16</b> AF-317J <b>17</b> 7 IV	13. NUMBER OF PAGES 38 <b>12</b> 40 p.	
	15. SECURITY CLASSIFICATION Unclassified	
	15a. DECLASSIFICATION/DOWNGRADING SCHEDULE	
16. DISTRIBUTION STATEMENT (of this Report) Distribution limited to US Government agencies only because of test and evaluation of military systems (Dec 75). Other requests for this document must be referred to AFWL (LRO), Kirtland AFB, NM 87117.		
17. DISTRIBUTION STATEMENT (of the abstract entered in Block 20, if different from Report)		
18. SUPPLEMENTARY NOTES		
19. KEY WORDS (Continue on reverse side if necessary and identify by block number) Actuators Electromagnetic Solenoid Pointing Optical		
20. ABSTRACT (Continue on reverse side if necessary and identify by block number) Recent Air Force contracts have identified the need for very high frequency response (700 Hz), high force level, linear actuators for use in wide bandwidth mirror positioning systems. This report describes testing performed on a linear-motion, bidirectional solenoid with a rated 52 pound continuous force capability. Testing included static force capability, linearity, heating, and dynamic force capability. Dynamic tests showed a 44:1 loss in force output from zero frequency to 500 Hz, and a phase lag of force with (OVER)		

DD FORM 1 JAN 73 1473

EDITION OF 1 NOV 65 IS OBSOLETE

UNCLASSIFIED

SECURITY CLASSIFICATION OF THIS PAGE (When Data Entered)

401 925

DN


OVER

UNCLASSIFIED

SECURITY CLASSIFICATION OF THIS PAGE(When Data Entered)

ABSTRACT (Cont'd)

respect to current that increased with frequency and with input current level. These characteristics make this actuator incompatible with the requirements for the desired wide bandwidth control loop.



UNCLASSIFIED

SECURITY CLASSIFICATION OF THIS PAGE(When Data Entered)

## PREFACE

Richard R. Auelmann was the project leader for the study described in this report; Harold W. Schaeffen was the principal investigator; Paul C. Kiumke was responsible for Mechanical Design; Peter Baldwin was responsible for Electronic Design.

## CONTENTS

<u>Section</u>		<u>Page</u>
I	INTRODUCTION AND SUMMARY	1
	Introduction	1
	Summary	3
II	STATIC TESTS	5
	External Characteristics	5
	Static Force Tests	6
III	DYNAMIC TESTS	17
	Current Drive Loops	17
	Test Setup	20
	Open Loop Tests	20
	Closed Loop Attempts	25



## ILLUSTRATIONS

<u>Figure</u>		<u>Page</u>
1	Position Loop Open Loop Response Goal	2
2	Cutaway View of Ledex Bidirectional Solenoid	3
3	Static Test Setup	7
4	Static Force Versus Current: Extend Coil	8
5	Static Force Versus Current: Retract Coil	9
6	Static Force for Small Currents: Extend Coil at Midpoint	11
7	Static Force for Differential Currents: Coils Nominally Biased at 5.5 Amperes	12
8	Magnetic Spring Characteristics: Force Versus Position	13
9	Actuator Heating Characteristics	15
10	LB-33 Coil Impedance Variation with Frequency: Biased at 5.5 Amperes, Referenced to 1.1 ohm (DC)	17
11	Differential Current Command Block Diagram	18
12	Current Drive Closed Loop Frequency Response	19
13	Linear Load Equivalency	21
14	Dynamic Test Setup	22
15	Actuator Force and Phase Variation with Frequency and Amplitude	24
16	Block Diagram: 350 Hertz Mirror Position Loop	27
17	Open Loop Response: 350 Hertz Mirror Position Loop	28
18	Block Diagram: 300 Hertz Mirror Loop with Integral Compensation	29
19	Open Loop Response: 300 Hertz Mirror Loop	31
20	Idealized Loop Resulting in Open Loop Gain "Goal"	32
21	High Frequency Compensation Gain Comparison	33

## SECTION I

### INTRODUCTION AND SUMMARY

#### 1. INTRODUCTION

Recent Air Force contracts, notably for the Airborne Pointing and Tracking (APT) system and the Large Pointing System (LPS), have shown a requirement for small, high force capability linear actuators. This requirement was met with hydraulic actuation on the APT system; hydraulic actuators were also included in the LPS design study effort.

Recently a new line of commercially available electromagnetic actuators was introduced by Ledex, Inc., Dayton, Ohio. These actuators are essentially dual solenoids providing bidirectional forces. The highest force capability unit, Model LB-33, can produce up to 100 pounds force. Very little data on frequency response characteristics of these actuators was available from the manufacturer. This task of the Large Pointing System contract was to purchase this actuator and perform those tests necessary to determine its applicability in a high force, high frequency response position control loop.

In the LPS, the autoalignment mirror must follow base motions and correct for high frequency pointing errors of other mirrors in the system. In order to satisfactorily perform this correction, a high bandwidth loop, with an open loop crossover near 500 Hz, is required. In particular, a control loop with open loop characteristics as shown in figure 1 is required. Thus the essential objective of this task was to determine if the LB-33 actuator could be configured into a control loop with characteristics similar to those shown in figure 1.

The actuator, Ledex model LB-33, is shown in a cutaway view in figure 2. The unit consists of two coils (extend coil and retract coil), specially shaped magnetic pole pieces, and an armature mounted on the shaft. The shaft is supported on Teflon coated bushings at either end of the actuator. As the extend coil is energized, the shaft moves toward the reader, independent of direction of current in the winding, i.e., the usual solenoid effect. The opposite motion is produced by energizing the retract coil. The specially shaped magnetic circuit results in a shaft force proportional to the current in the windings. The

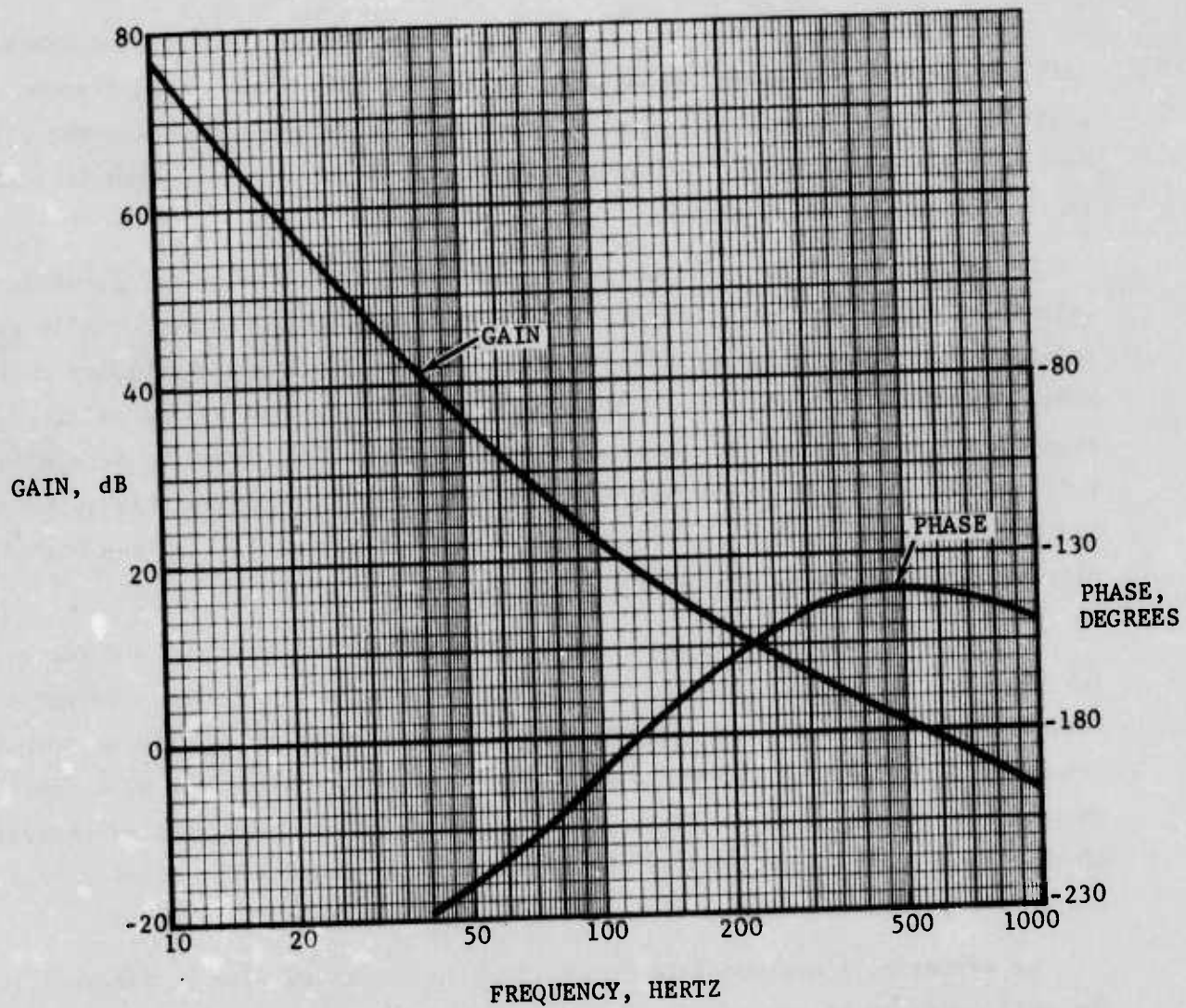


Figure 1. Position Loop Open Loop Response Goal



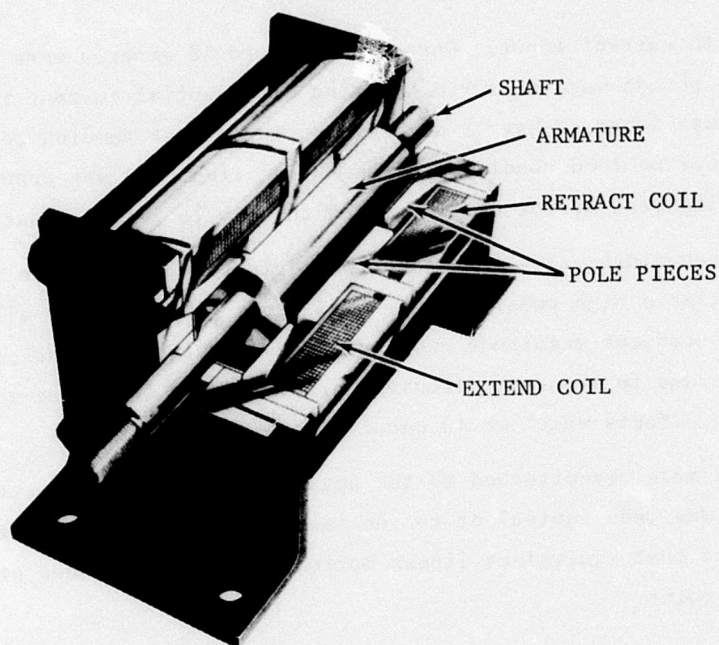


Figure 2. Cutaway View of Ledex Bidirectional Solenoid

unit purchased had an integral linear feedback potentiometer mounted to the far end (shown without threads) of the shaft and housing.

## 2. SUMMARY

Acceptance testing of the actuator consisted of static measurements of force versus coil current. The first unit delivered showed a force output drastically below the nominal level and was also very nonlinear, with force varying more like the square root of current. This unit was returned to Ledex for rework. Upon its second delivery, acceptance tests showed the proper force output and linearity; therefore, testing proceeded as planned.

Preliminary testing included external characteristics such as winding resistance, shaft friction, potentiometer resistance and noise, stroke capability and weight. Static tests were then performed to evaluate force output due to each coil, force output for coil differential currents, linearity, and heating characteristics. The actuator exhibited better than rated force output over its entire stroke length; above approximately 0.5 ampere, force output was quite

linear with current input. Currents of up to 18 amperes were used and forces up to 110 pounds were measured. During differential current testing, the actuator was found to have a magnetic spring effect tending to center the armature. Under no load conditions, the spring frequency was around 40 Hz. In the LPS autoalignment mirror configuration this would become about 10 Hz.

Wide bandwidth, closed loop current drive amplifiers were designed and built using available high power voltage amplifiers. These loops allowed the use of controlled current magnitude and waveshapes at high frequencies, eliminating distortion due to magnetic circuit characteristics and force fall-off due to inductance effects which would occur with a voltage drive.

A load mass was attached to the actuator for dynamic measurements. This load mass was made equivalent to the inertia of the LPS autoalignment mirror assembly so that equivalent linear motions would be produced at each force and frequency point.

An accelerometer was mounted on the load mass so that the actuator force output over the frequency range of interest could be measured. Constant value sinusoidal currents were induced in the windings while force and force-to-current phase angle were measured over a range of 10 to 600 Hertz. The actuator proved to have a substantial loss in force capability at high frequencies. The force output per unit differential current input decreased from 6 pounds per amp at 10 Hz and below to 0.14 pounds per amp at 500 Hz. Phase lag between force and current was present, increasing both with frequency and with magnitude of input current.

Attempts were made to operate the actuator in a closed position loop, and a loop of approximately 350 Hz open loop crossover was closed. This loop was difficult to stabilize due to the force and phase characteristics of the actuator. The open loop gain characteristics of the loop fell far below the desired goals. Further control loops were configured, but due to the compensation required for the actuator characteristics, no workable loop close to the goal appears possible with this actuator.

In summary, because of the degradation in force and phase characteristics of this actuator at high frequency, it cannot be considered a viable candidate for autoalignment mirror actuation in any wide bandwidth control loop.



## SECTION II

### STATIC TESTS

This section describes all tests performed on the actuator under static conditions.

#### 1. EXTERNAL CHARACTERISTICS

Table 1 includes all pertinent actuator parameters known or measured upon receipt of the actuator.

Table 1  
ACTUATOR CHARACTERISTICS

Weight, pounds	12 (approx)
Size: inches	
Length	11.4 (including feedback potentiometer)
Height	4.13
Width	3.38
Travel, inches	0.14 (0.125 rated)
Coil resistance, ohms	
Extend coil	1.10
Retract coil	1.10
Feedback potentiometer (Conductive plastic, infinite resolution)	
Total resistance, ohms	5000
Variation, extend-retract, ohms	700
Breakaway friction, ounces	
Horizontal Extend	6.0
Retract	6.0
Vertical Extend	2.0
Retract	2.0
Magnetic breakaway friction, ounces	2.0 to 6.0

The coulomb friction was measured with no current to the actuator. The additional friction measured with current in the coils is approximate because of the method of measurement which relied upon the linearity of the force/current relationships. Noise on the potentiometer was measured through observation of the pickoff voltage on an oscilloscope and was found to be the equivalent of 5 to 10 microinches of travel. Based on this measurement it was decided to use the linear potentiometer for the feedback element for later closed loop tests.

## 2. STATIC FORCE TESTS

### a. Test Setup

Figure 3 shows the actuator, test fixture, and mechanical measuring device used for static force measurements. The position transducer (linear potentiometer) was used to monitor shaft position. The force transducer was an Ormond force gauge with a range  $\pm 1000$  pounds. Some tests were also performed with a low range ( $\pm 25$  pound) scale to adjust for small ( $\pm 3$  pound) hysteresis in the Ormond gauge tests. Also shown in figure 3 are the cutoff leads from the thermocouples which were used for heating tests. These thermocouples were welded to the actuator case over the middle of each coil.

### b. Force Versus Current

Basic static force versus current tests were performed on each coil for three different armature positions: extended, near mid-position, and retracted. The purposes of the tests were to determine force gain constant, linearity, and force variation with position.

Figure 4 shows results for the extend coil at the three positions. Each set of data is quite linear, and the force is seen to increase as the armature is displaced from the coil, i.e., forces are lowest for the extend coil when the armature is extended, or more centered in the extend coil. These curves show a slope of approximately 6 pounds per ampere.

Figure 5 shows the equivalent curves for the retract coil. Similar observations may be made; again the slope is approximately 6 pounds per ampere. The test data were obtained by taking readings while stepwise increasing current, then decreasing current from the maximum, then averaging the two readings

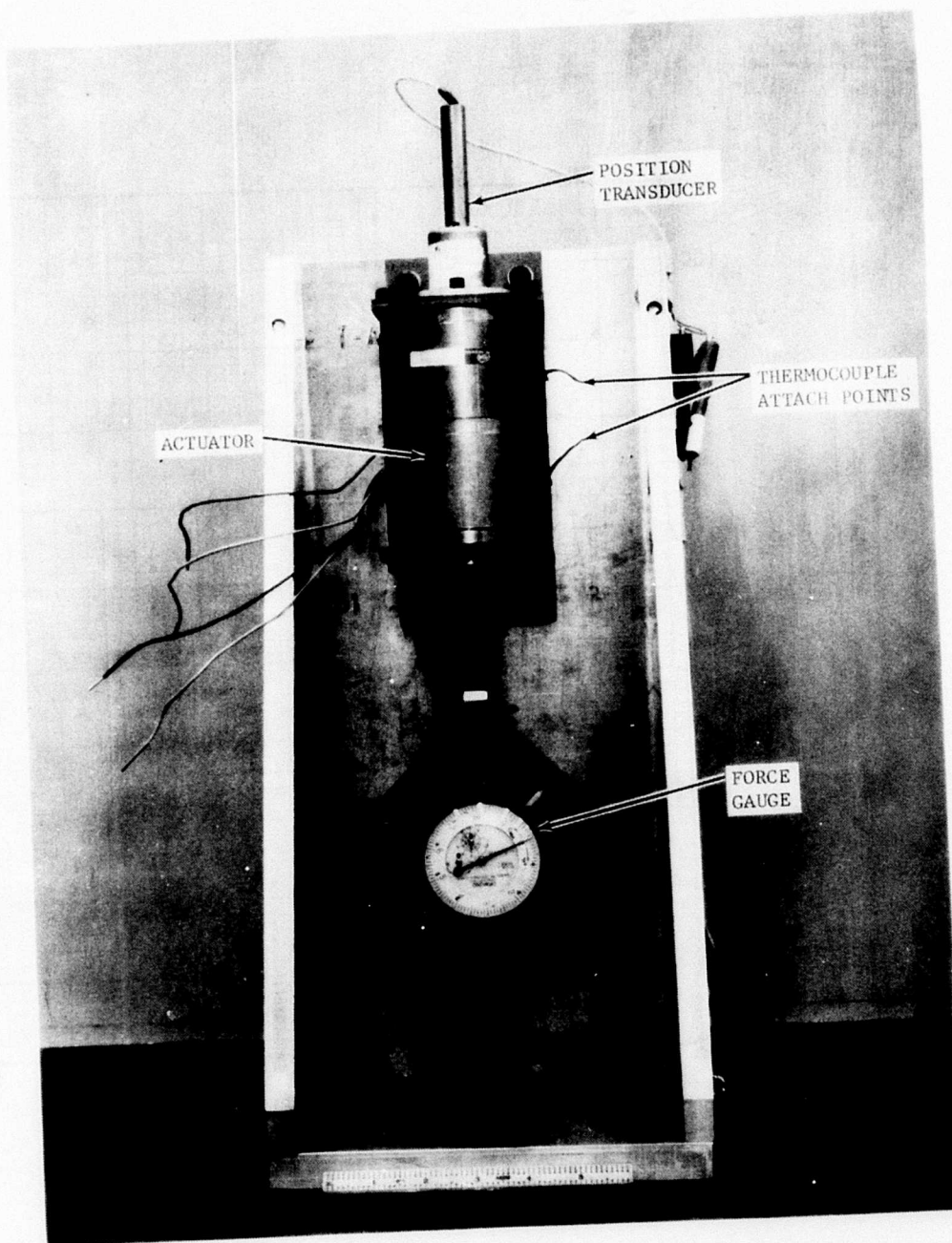


Figure 3. Static Test Setup



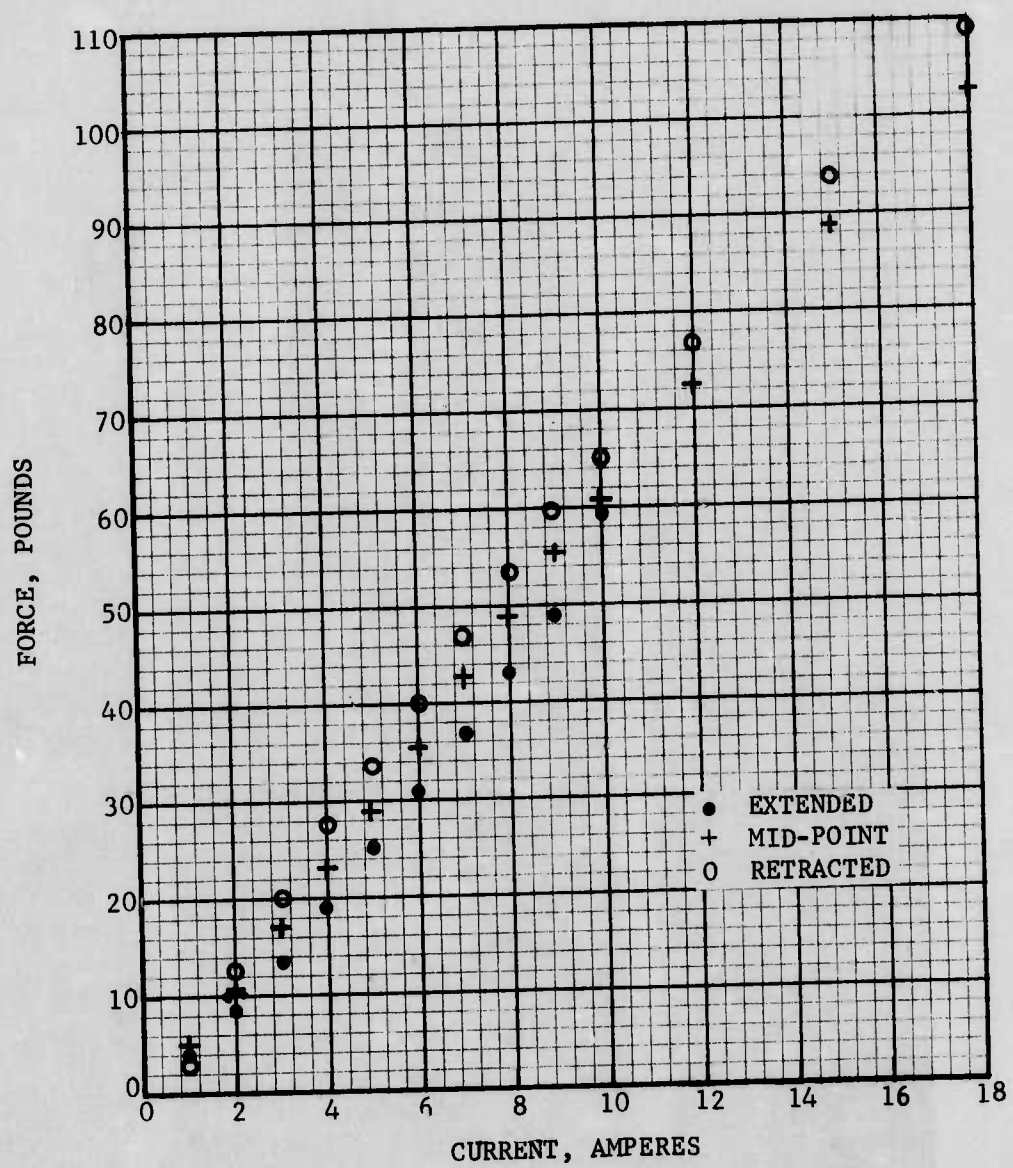


Figure 4. Static Force Versus Current: Extend Coil

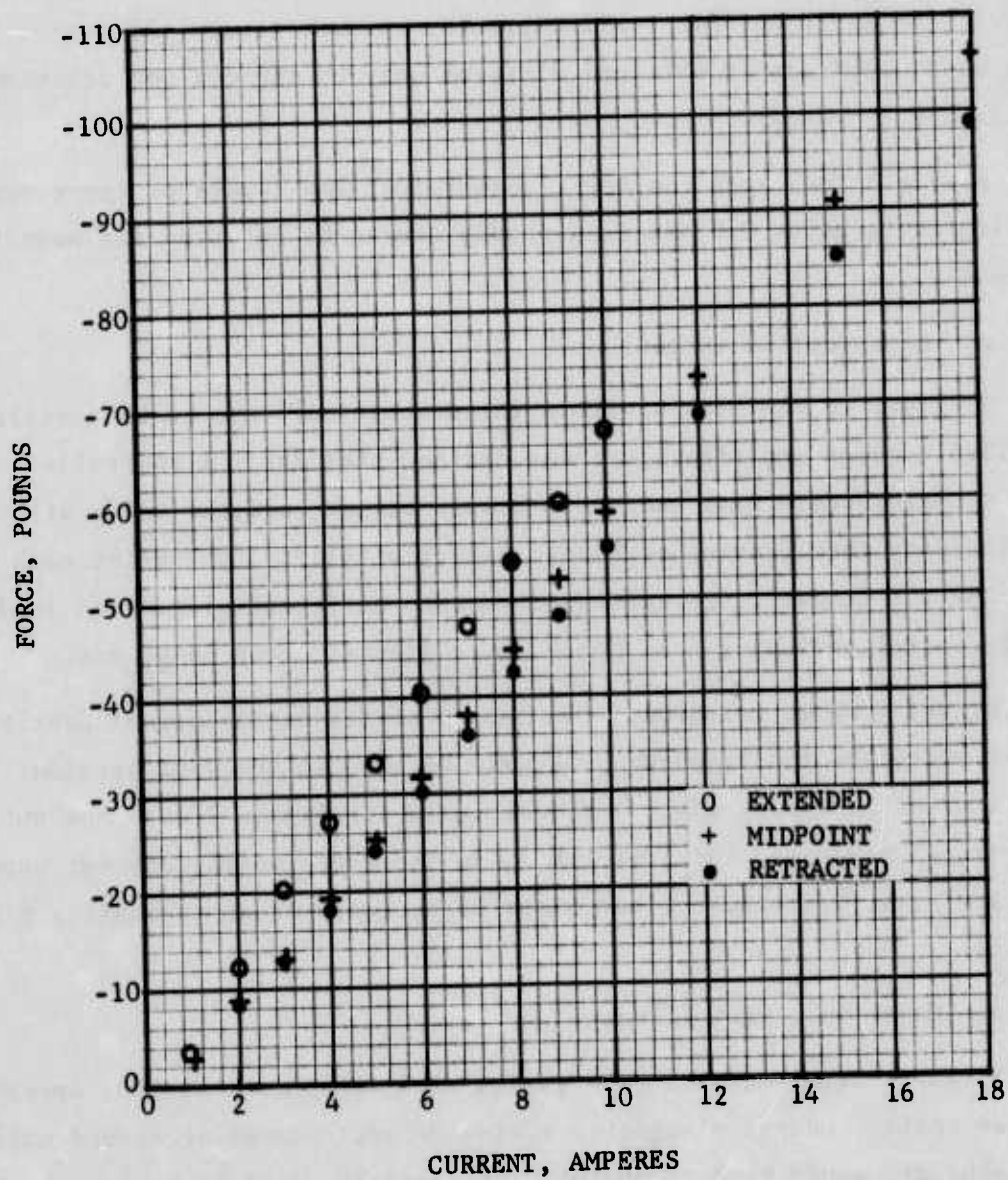


Figure 5. Static Force Versus Current: Retract Coil



for each current level to minimize the affect of the force gauge hysteresis and coulomb friction. Data points shown are the averaged readings. In order to assure that the actuator itself did not exhibit major hysteresis effects, other data were taken. One method was to tap the force gauge while taking readings; the readings so obtained differed essentially only by the coulomb friction level. In addition, for small currents, a lower level ( $\pm 25$  pound) force gauge was used; readings so obtained differed only by the coulomb friction level (0.5 to 0.75 pound).

Figure 6 indicates the force measured at low levels of input current. The nonlinearity below 0.6 amp is probably caused by friction and magnetic circuit effects.

#### c. Differential Current

In order to minimize nonlinearities about null and to best utilize the available power amplifiers, it was decided that for all controlled operations, the actuator would have each coil biased at some nominal value with force obtained by then driving each coil differentially. By biasing each coil at 5.5 amps, a linear range extends from zero differential current to 11 amps differential, allowing peak force up to approximately 65 pounds.

Figure 7 shows measured force versus differential current near the nominal mid-position of the actuator. As will be seen in the next section, the actuator had a magnetic spring effect; because data for figure 7 were not obtained at the electrical midpoint, there is a bias to the force versus current curve due to the spring effect. Again, the slope of the data is approximately 6 pounds per ampere.

#### d. Magnetic Spring Effect

Because force for each coil varies with armature position, operating with biased coils produces a magnetic spring effect; operating around null current in each coil would tend to minimize the spring effect by making the force variation appear as a nonlinear gain. Results of some force variation tests with armature position and current are shown in figure 8. The middle curve shows force versus position with equal 5.5 amps currents in each coil. The upper curve shows results for 7.0 amps in the extend coil and 4.0 amps in the retract

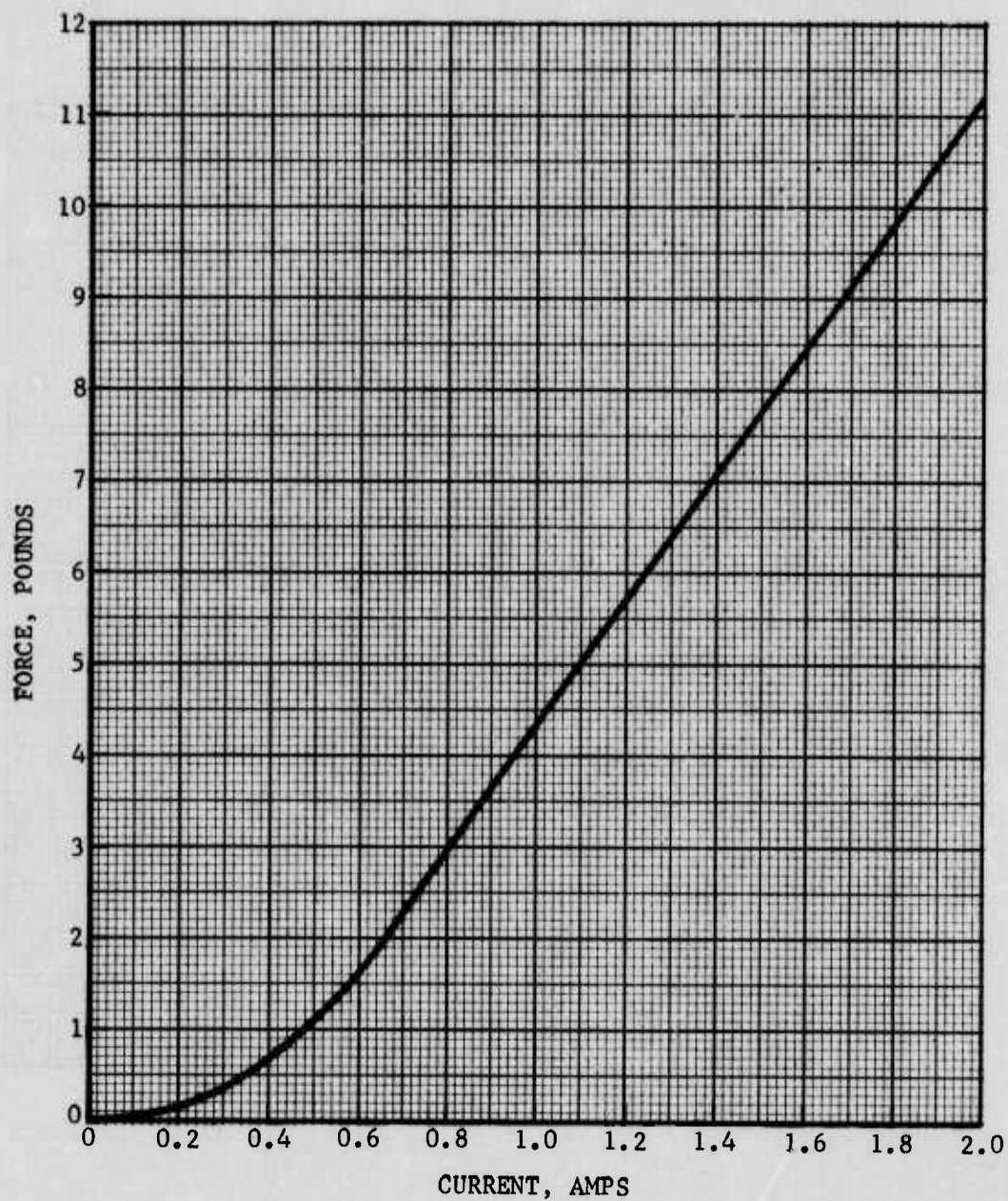


Figure 6. Static Force for Small Currents: Extend Coil at Midpoint

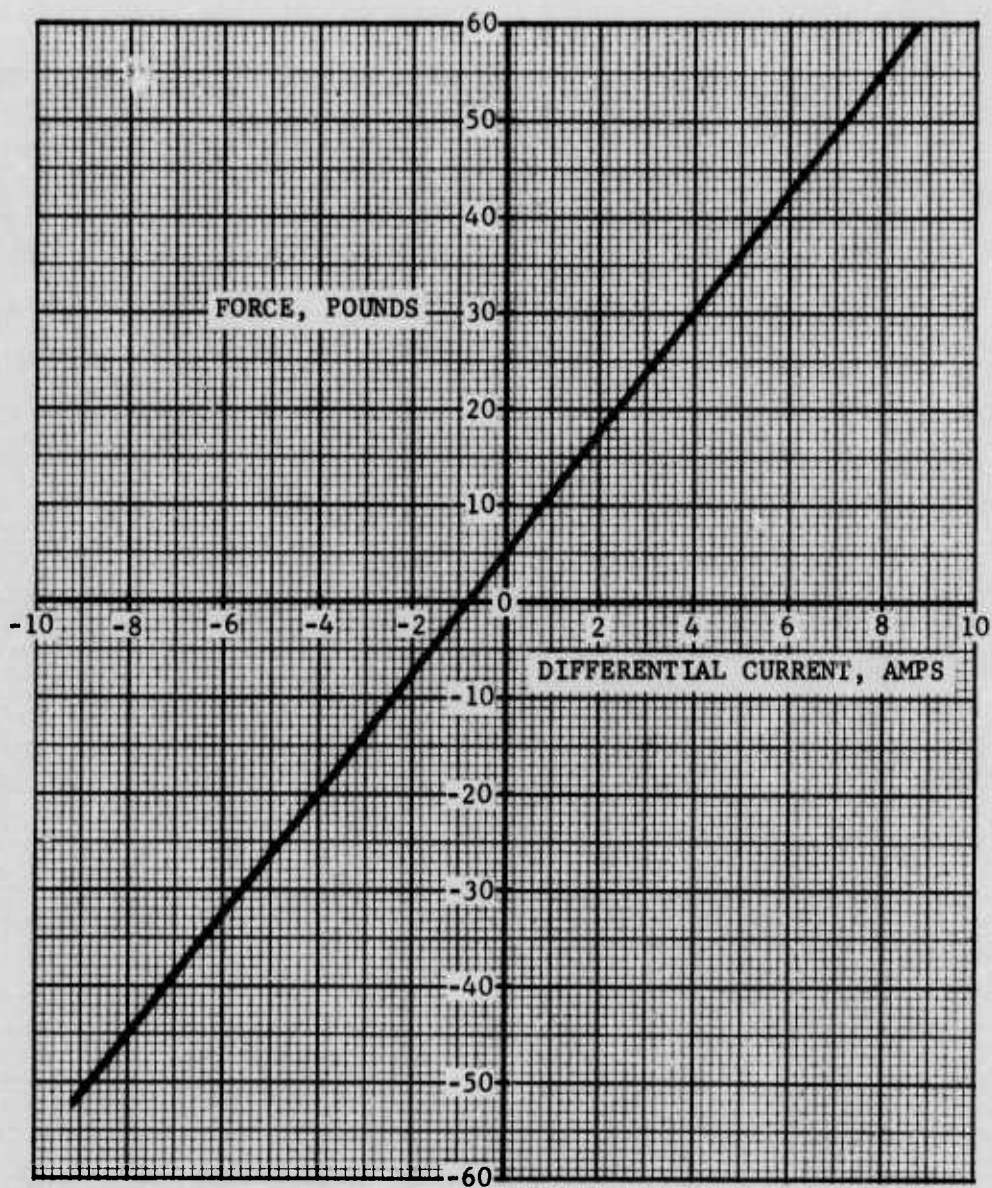


Figure 7. Static Force for Differential Currents:  
Coils Nominally Biased at 5.5 Amperes



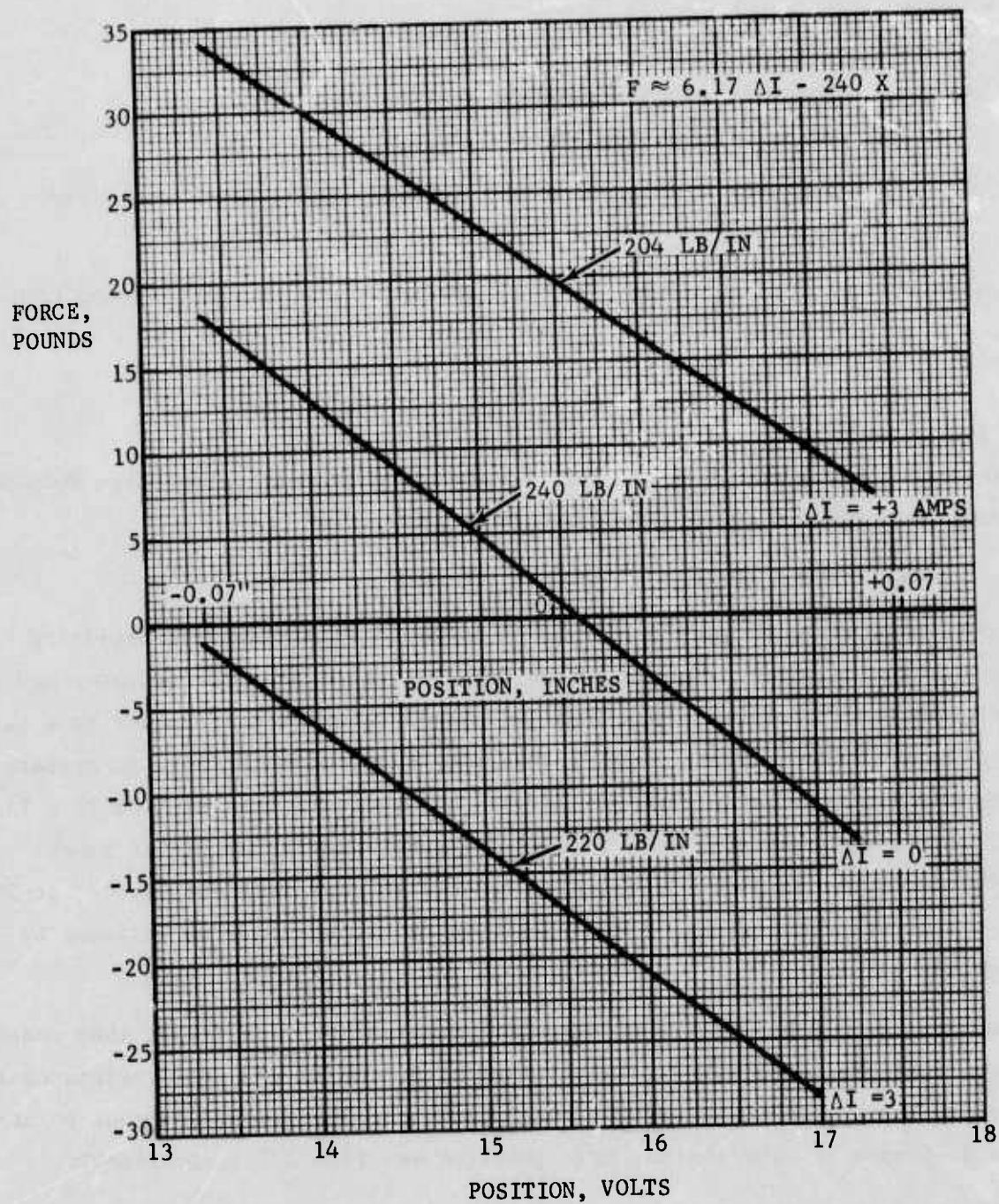


Figure 8. Magnetic Spring Characteristics: Force Versus Position

coil for a differential current of 3.0 amperes; the lower curve with 7.0 amperes retract, 4.0 extend. A reasonable static force equation for the actuator acting with biased coils is:

$$F = 6.17 \Delta I - 240X$$

where  $F$  = force in pounds, positive tending to extend

$\Delta I$  = coil differential current,  $I_{\text{EXTEND}} - I_{\text{RETRACT}}$

$X$  = armature displacement from magnetic null, inches, positive extending.

With the unloaded actuator, 24 ounce armature, the magnetic spring frequency is

$$f = \frac{1}{2\pi} \sqrt{\frac{240}{0.00388}} = 39.6 \text{ Hz}$$

In the later tests with a load mass corresponding to use in the Large Pointing System, the magnetic spring frequency is 9.33 Hz.

#### e. Coil Heating Tests

Coil heating tests were performed in order to determine safe operating times for the actuator. Manufacturers data indicated that the actuator had a safe upper limit coil temperature of  $150^{\circ}\text{C}$  ( $302^{\circ}\text{F}$ ) which corresponds to a case temperature of  $90^{\circ}\text{C}$  ( $194^{\circ}\text{F}$ ). The actuator is supposed to be able to operate continuously at 145 watts dissipation when mounted on a heat sink of 12 x 12 x 1/8-inch aluminum plate, in a  $25^{\circ}\text{C}$  ( $77^{\circ}\text{F}$ ) environment. At higher power dissipations, the actuator is rated to be able to sustain a duty cycle; at 290 watts, for example, the duty cycle rating is 72 seconds on time followed by 72 seconds off time.

Aeronutronic tests were conducted with constant current rather than constant power; therefore the dissipation increased with time as the coil resistance increased. Case temperature was monitored using the thermocouple attach points shown in figure 3. The thermocouple junction was Type J Iron-Constantin.

Figure 9 shows the results of the heating tests performed. The first test was at the nominal bias point to be used in subsequent tests, 5.5 amps per coil. This test had a dissipation of 67 watts at the beginning. The test was terminated at 17 minutes with a case temperature of  $100^{\circ}\text{F}$ ; power dissipation was



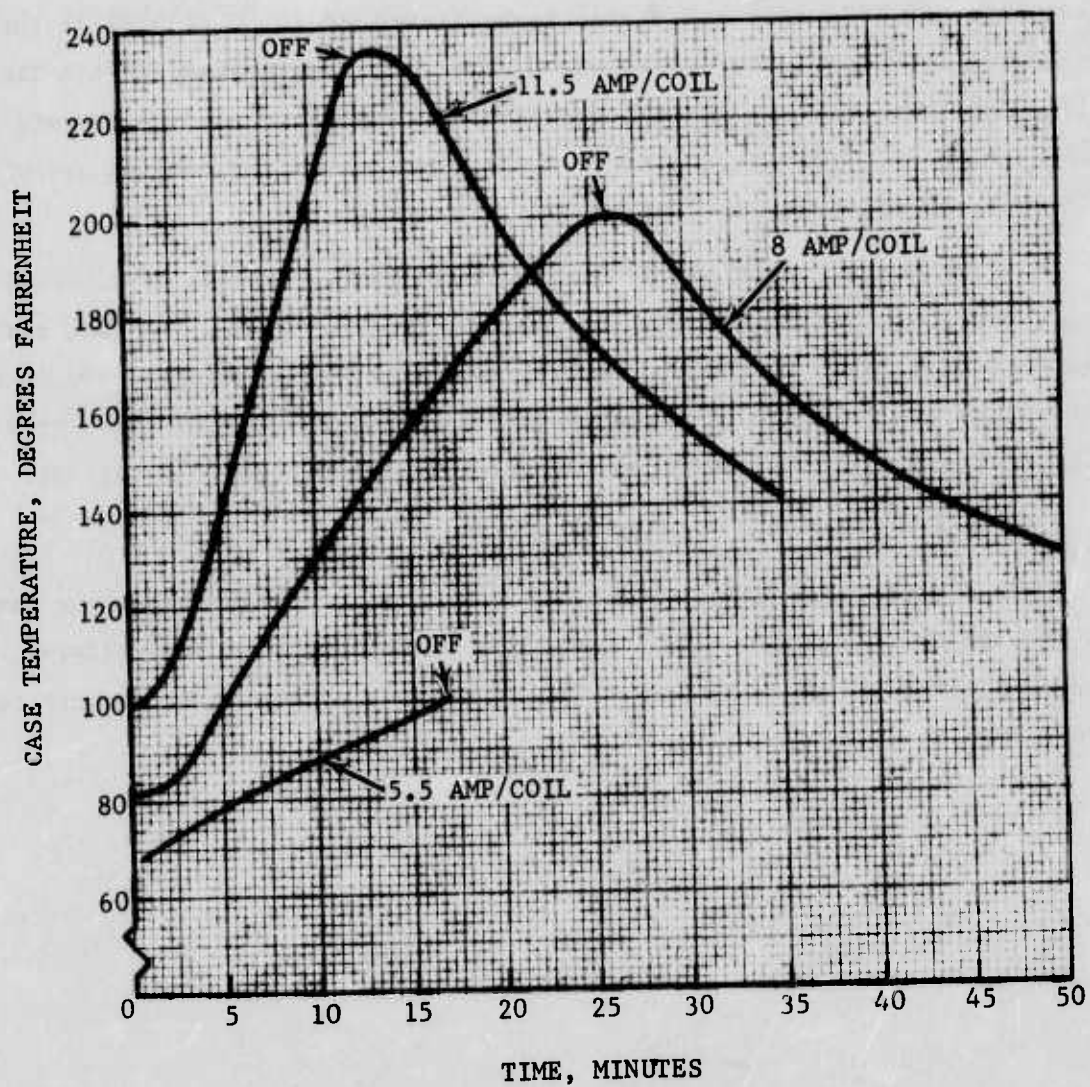


Figure 9. Actuator Heating Characteristics

small compared to rated dissipation, making this test somewhat uninteresting except to show that temperature rise at the nominal bias point was low. Next a constant 8 amperes was used in each coil; at room temperature this represents 141 watts dissipation. After 25 minutes at constant current the case temperature reached its nominal limit of 200°F, and the actuator was turned off. Coil resistance measurements showed a resistance of 1.55 ohms, indicating a power dissipation of 198 watts and a coil temperature\* of 115°C (239°F) at turn-off. This curve represents the worst case dissipation when operating with biased coils, and shows that at maximum force output the unit could be operated longer than 25 minutes. The continuation of the curve shows the cooling cycle in a 75°F ambient, no forced cooling.

The last heating test was 11.5 amperes per coil; initial dissipation at room temperature would have been 291 watts. In 9.5 minutes the case temperature rose from 100°F to 200°F. When turned off after 12 minutes the case temperature was 235°F; resistance measurements indicated 2.07 ohms for a final power dissipation of 547 watts and a coil temperature of 225°C (437°F).

#### f. Force at Elevated Temperatures

Force versus current tests were run with case temperatures in the range of 120° to 150°F, with no loss in force output with increased temperature. Of course, because of the increased coil resistance, higher voltages were required to produce the currents.

---

\*where  $R' = R(1 + 0.0043(T - 20^{\circ}\text{C}))$

### SECTION III

#### DYNAMIC TESTS

The purpose of this section is to present the results of all the dynamic tests, or those tests with sinusoidal drive currents and/or moving armature. It describes the design of the current drive loops, test setup, open loop measurements and closed loop results. In contrast to the static tests, wherein the actuator produced the desired force levels, the dynamic test results are disappointing and show that this actuator, in its present form, is not a viable candidate for a 500-Hz control loop. Comments based on conversations with the manufacturers (Ledex) engineers as to the reason for the results are included below.

#### 1. CURRENT DRIVE LOOPS

##### a. Coil Impedance Measurement

The first step in forming the current drive control loops was to measure the actuator coil impedance characteristics. This was done by imposing a static 5.5 ampere bias and a 0.2-ampere peak-to-peak sinusoidal current and measuring the required sinusoidal voltage and voltage-to-current phase. Results of these measurements are shown in figure 10. Gain is shown as:  $\text{Gain(dB)} = 20 \log(Z/1.1)$ .

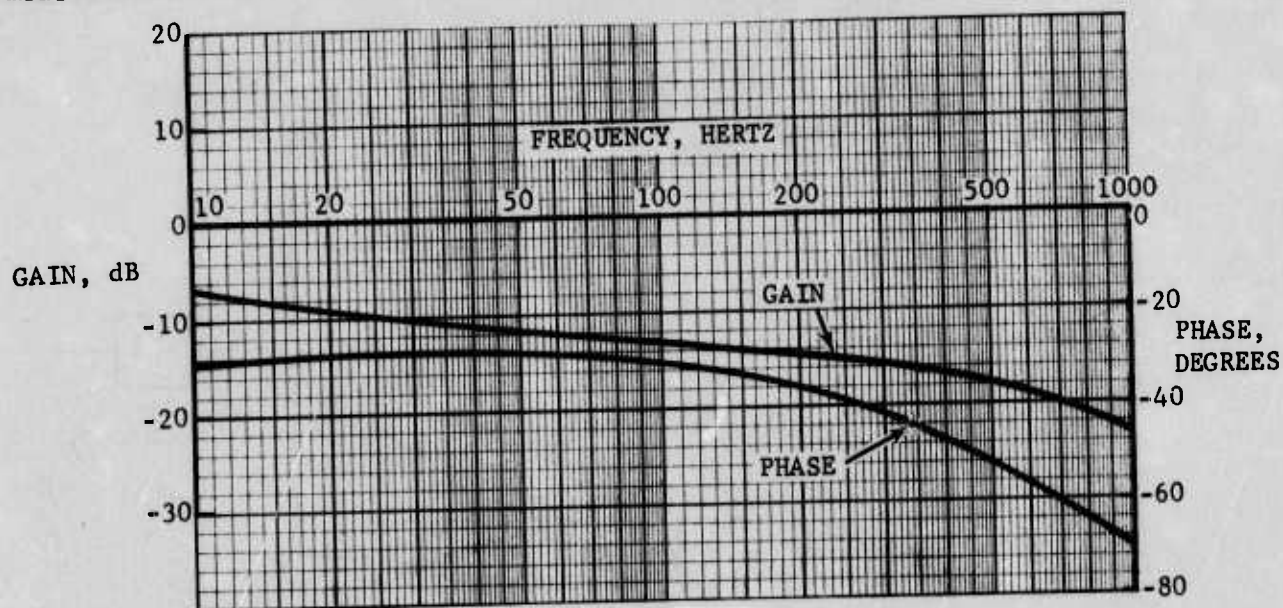


Figure 10. LB-33 Coil Impedance Variation with Frequency:  
Biased at 5.5 Amperes, Referenced to 1.1 Ohms

No attempt was fruitful in explaining the high frequency characteristics; they were accepted and incorporated into the current drive loop. Prior to these measurements the coil characteristics were expected to be a 1.1-ohm resistance and an inductance on the order of 0.07 henry. If a series resistance-inductance model is assumed, the measurement data shown in figure 10 indicate the following: at 10 Hz,  $R = 2.16$  ohms,  $L = 0.02$  henry; at 100 Hz,  $R = 4.9$  ohms,  $L = 0.0023$  henry. High frequency impedance was much lower than expected; thus, with the available amplifiers, more current than was expected could be attained at high frequency.

#### b. Current Drive Response

The differential current drive control block diagram is shown in figure 11. Two control loops are used, one for each coil. Each coil is biased at 5.5 amps with the command adding to one coil, subtracting from the other. The available power amplifiers were voltage amplifiers; the loops were closed using a current sensing resistor and compensation to increase gain and compensate for the coil impedance characteristics. Frequency response of the closed current loop is presented in figure 12. Only 12 degrees phase lag is exhibited at 500 Hz.

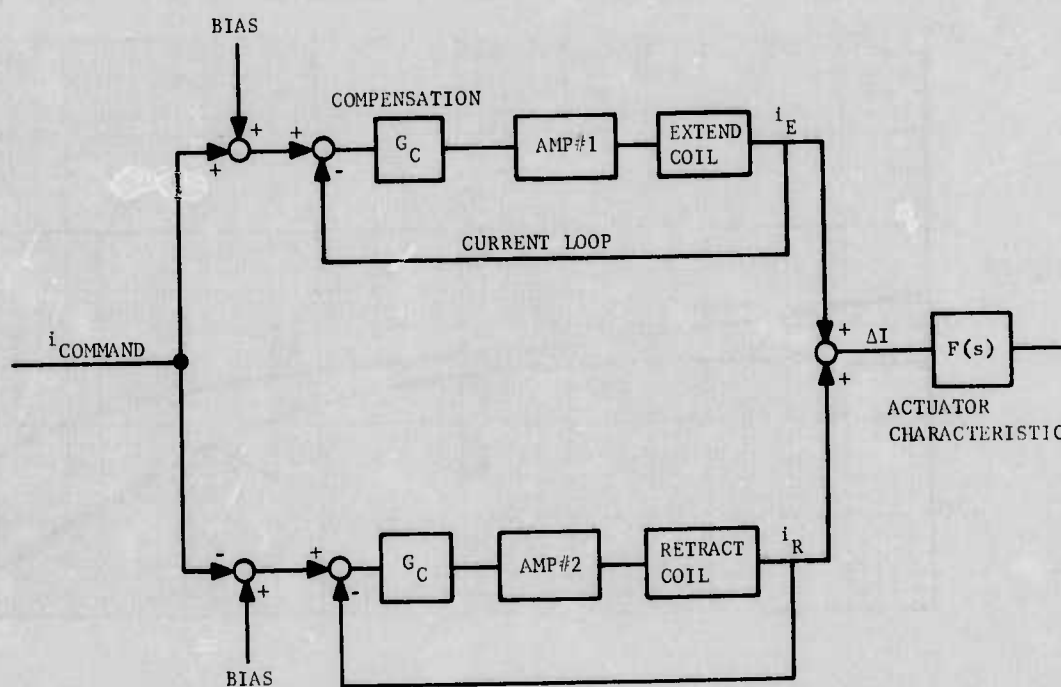


Figure 11. Differential Current Command Block Diagram



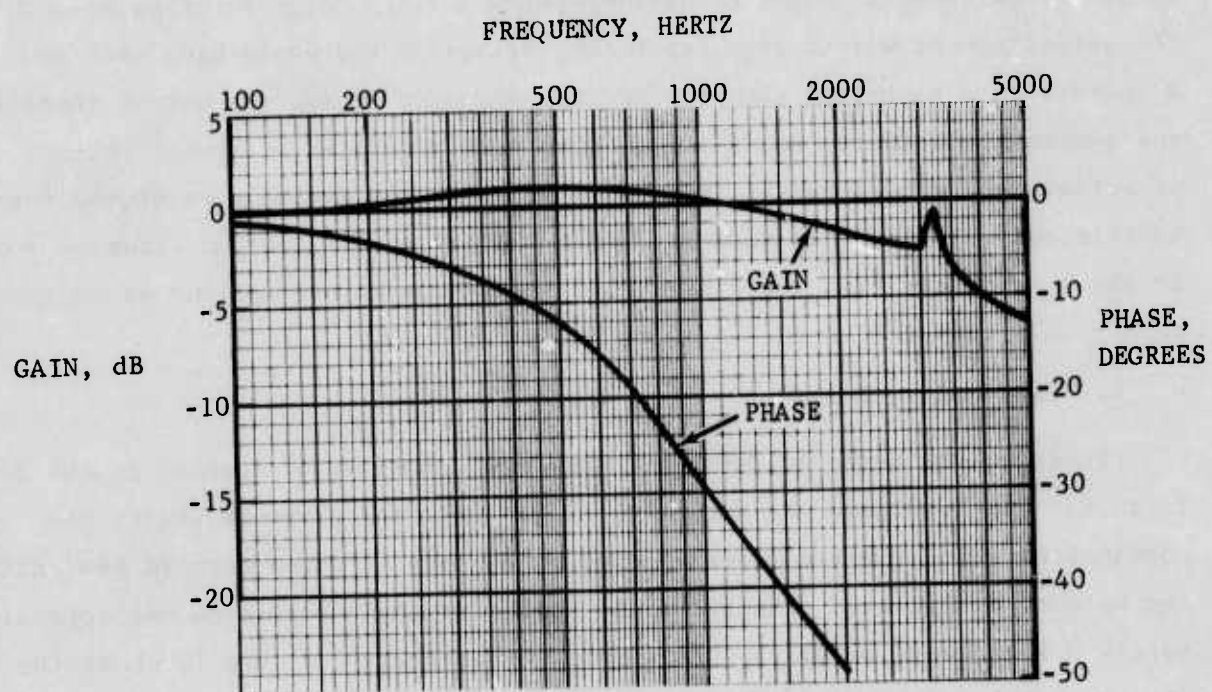


Figure 12. Current Drive Closed Loop Frequency Response



Each amplifier had the capability to drive 4 amps peak-to-peak at 500 Hz, for a differential current of 8 amps peak-to-peak in the actuator; the full 11 amp peak-to-peak differential current could be attained up to 300 Hz.

## 2. TEST SETUP

### a. Load Mass Equivalent

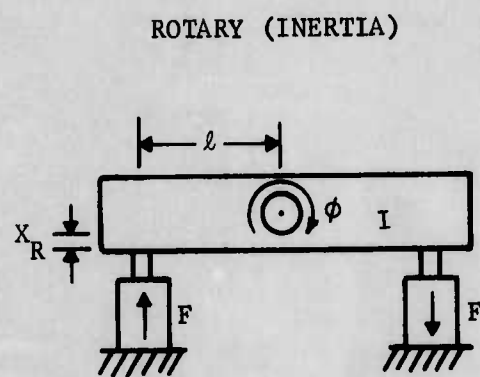
The objective of the actuator testing was to determine its applicability to the autoalignment mirror actuation system for the Large Pointing System (LPS). The autoalignment mirror requires rotary actuation and would have used two actuators in a push-pull manner. For the actuator tests, the mirror inertia and consequent actuator loads and motions were simulated by linear motions of an actuator-load mass setup. Figure 13 presents the equivalency of the mass/inertia and actuator displacements under the basic rule that an actuator force in the linear test case would result in the same armature motions as in the rotary (LPS) case.

### b. Test Configuration

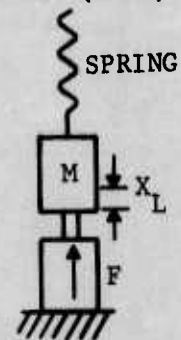
Figure 14 shows the actuator and load mass combination mounted in the test fixture. The load mass was securely screwed onto the armature shaft; the combination mass-armature was suspended on 8 feet of bungee cord to neutralize the effects of gravity. The spring frequency of the combination was approximately 0.6 Hz, well below the frequencies of interest. Figure 14 shows the fixture firmly attached to the concrete floor. The static test setup photo, figure 3, shows the position transducer mounted to the actuator case. As shown in figure 14, this mounting was changed to mount the position transducer to the fixture. This was done in order to eliminate false motion indications if the actuator case rather than armature moved. An Endevco model 2246 piezo-electric accelerometer is shown mounted on the top of the load mass. This accelerometer, mated to an Unholtz-Dickie model 8PMCV charge amplifier has a flat frequency response from 20 Hz to well over 5000 Hz, thus giving very good measurements of load motion in the 100-500 Hz band of interest.

## 3. OPEN LOOP TESTS

Prior to making any open loop dynamic measurements, several attempts were made to close a simple position control loop around the actuator. This loop was designed on the assumption that force/current ratio was constant with frequency



LINEAR (MASS)



$$\frac{2Fl}{I} = \ddot{\phi}$$

$$l\ddot{\phi} = \ddot{x}_R = \frac{2Fl^2}{I}$$

$$I = 3.3 \text{ IN-LB-SEC}^2$$

$$l = 5 \text{ INCHES}$$

$$\ddot{\phi} = 100 \text{ RAD/SEC}^2 \text{ AT } F = 33 \text{ LB}$$

$$\ddot{x}_R = 500 \text{ IN/SEC}^2$$

$$\frac{F}{M} = \ddot{x}_L$$

$$\ddot{x}_L \Leftrightarrow \ddot{x}_R$$

$$M = I/2l^2$$

$$M = 0.066 \text{ LB-SEC}^2/\text{IN}$$

$$W = 25.5 \text{ LB}$$

$$\ddot{x}_L = 500 \text{ IN/SEC}^2 \text{ AT } F = 33 \text{ LB}$$

Figure 13. Linear Load Equivalency

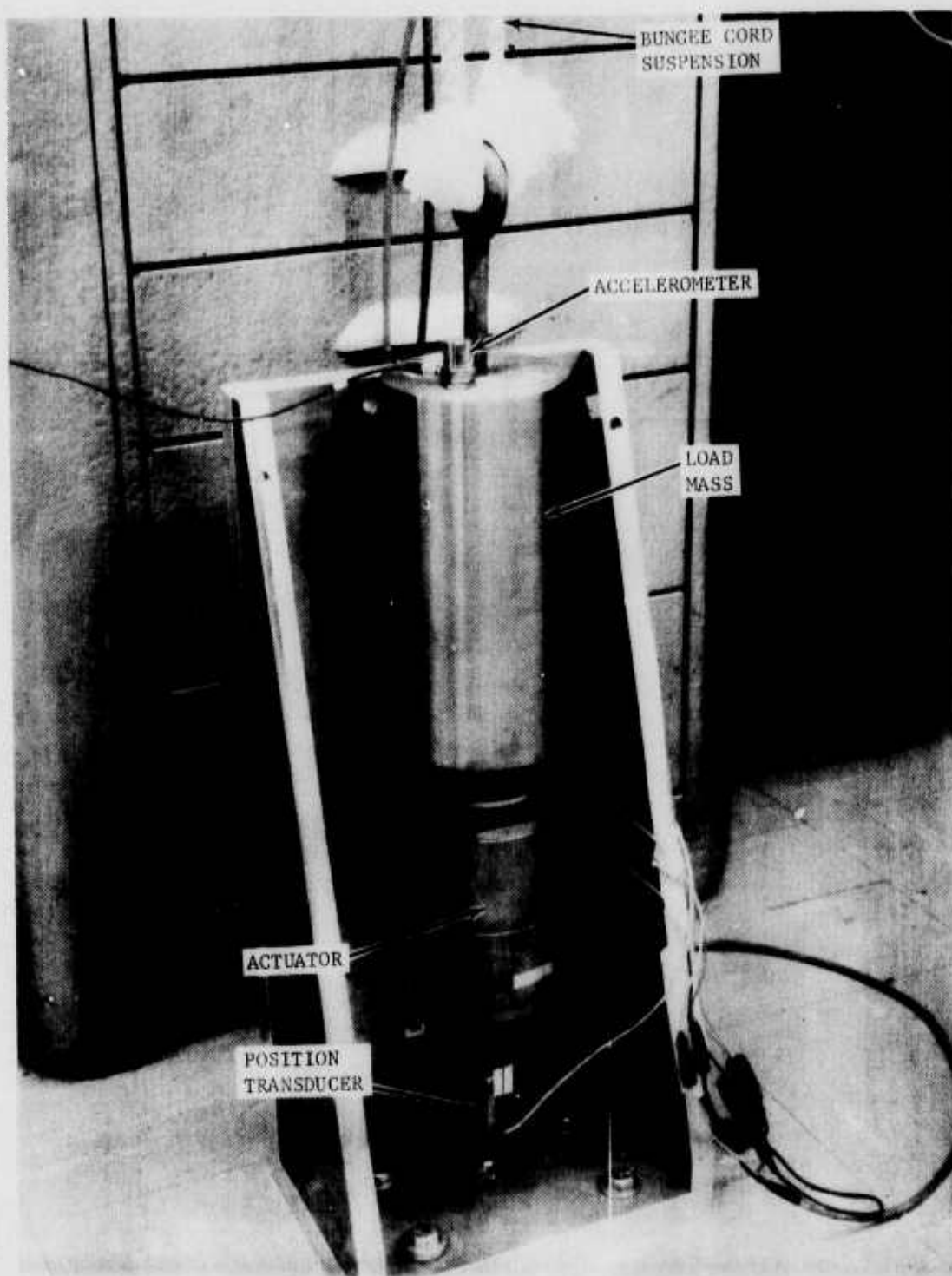


Figure 14. Dynamic Test Setup

and that there was no appreciable phase lag characteristics. All attempts at such a loop closure failed, and testing of the actuator to determine its frequency response characteristics in an open loop manner were initiated.

a. Procedure

The test setup shown in figure 14 was used. Sinusoidal current commands were input to the current drive loops shown in figure 11. Acceleration and position measurements were taken at various frequencies and current amplitudes; the accelerometer and position transducer outputs were observed on an oscilloscope and a wave analyzer was used for amplitude and phase measurements. The tests were repeated four times using two different accelerometers, with essentially the same acceleration and phase measurements obtained each time.

b. Test Results

Gain and phase measurements are presented in the Bode plot of figure 15; plots are shown of data taken with 1 and 5 ampere (zero to peak) commands. Gain is normalized to a 1 ampere sinusoidal command, or 2 amperes peak differential current. From the static tests, the nominal force expected is 12.34 pounds. Force values were obtained using acceleration measurements and converting by the spring/mass model:

$$F = (\text{Weight})(\text{"G"Reading}) \frac{(s^2 + 45.24s + 3571)}{s^2}$$

Phase was corrected for the spring/mass model at low frequency and for amplifier lags (figure 12) at higher frequencies.

Several important facts should be noted from figure 15. The most obvious is the significant force degradation as frequency is increased, from a capability of 12 pounds per ampere at low frequencies to 0.27 pound per ampere at 500 Hz, or a 44:1 loss in gain. At the higher frequencies (above 100 Hz), gain tended to decrease with amplitude also. The measured force exhibited a phase lag with respect to current which varied not only with frequency, but with amplitude.

Judged against the a priori assumption that force and phase angle would not vary with frequency or amplitude, these results are very disappointing. It must be remembered, however, that this was the object of performing these tests: to



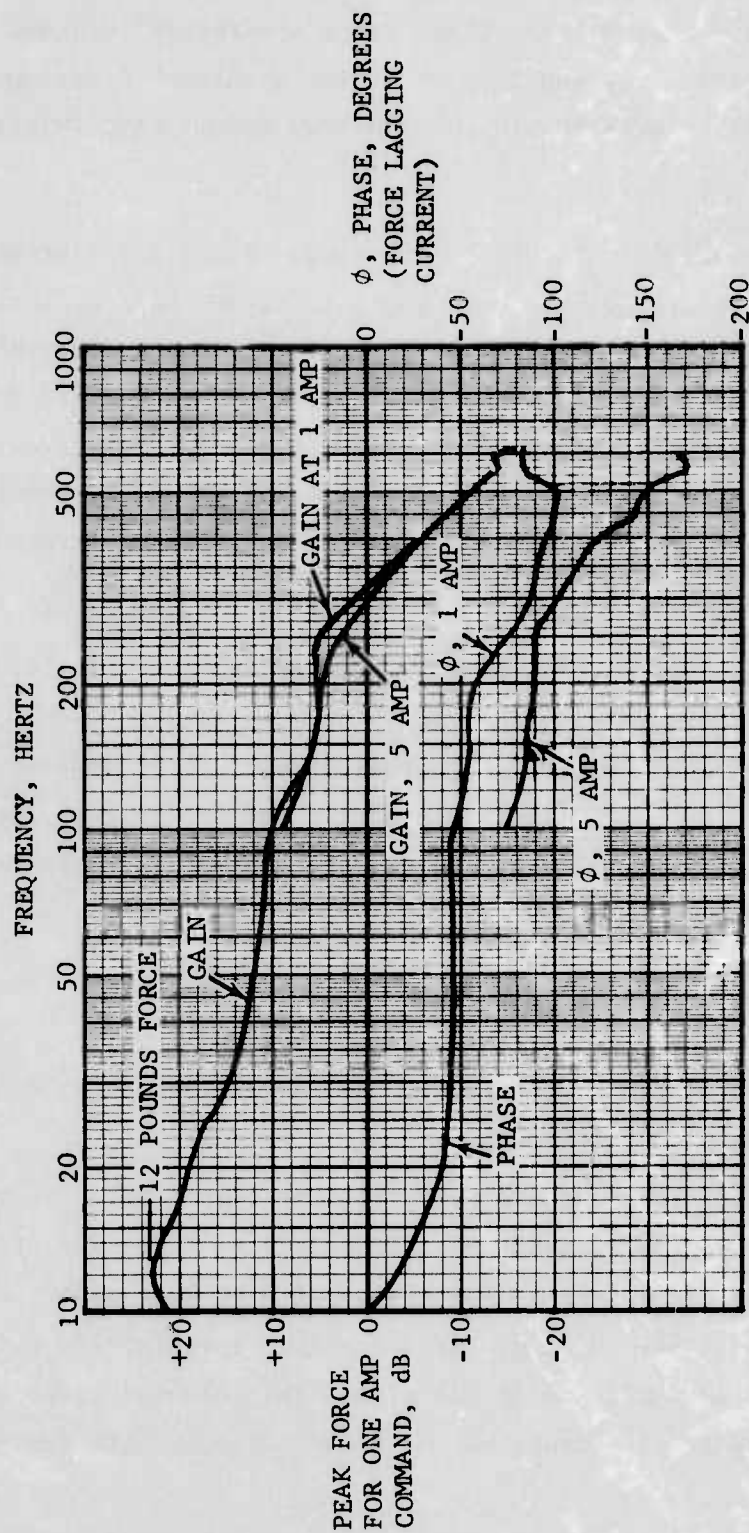


Figure 15. Actuator Force and Phase Variation with Frequency and Amplitude

determine how well the actuator would perform at high frequency, with no manufacturers data available.

Brief discussions were held with Ledex representatives concerning the force falloff with frequency. They stated that they had never made measurements as we did because the actuators are normally used in conjunction with a Ledex controller, which results in a relatively low frequency position loop. They also said that the force falloff could be attributed to three main causes: (1) eddy current losses because the magnetic circuit is solid, not laminated; (2) skin effect at high frequencies wherein the full volume of the magnetic circuit is not used, and (3) a "shorted turn" effect because the coils are wound on aluminum bobbins rather than non-conductive bobbins. They expressed interest in our test results, with a view towards possible modifications to improve the frequency response.

#### c. Other observations

During the open loop measurements, data were taken of the acceleration and displacement of the load mass. First displacement measurements were taken with the linear potentiometer supplied with the actuator and mounted to the actuator case. Displacement measurements correlated well with acceleration up to only 70 to 80 Hz. At high frequencies the potentiometer indicated more displacement than expected, up to three times the expected displacement at 120 Hz. "Expected" is calculated from  $x = \ddot{x}/\omega^2$ . Thinking that case motion might be causing erroneous potentiometer readings, the potentiometer was remounted to the fixture rather than the actuator case. Later tests with the fixture-mounted potentiometer indicated that the fault was in the potentiometer rather than the mounting.

A DC Linear Motion Transducer (Model SS-151) was obtained for engineering tests on consignment from G. L. Collins Company. This transducer is a linear variable differential transformer (LVDT) with integral oscillator/demodulation circuitry. Under tests similar to those above, this transducer produced measurements which correlated with acceleration up to around 300 Hz. This transducer was then used in subsequent closed loop tests.

#### 4. CLOSED LOOP ATTEMPTS

Although the actuator force test results indicated that a high frequency loop would be extremely difficult to implement, such attempts were made. The general philosophy was to try to compensate for all the bad characteristics of

the actuator and try to make the best loop with it. Numerous attempts were made, but only two are shown here in detail. The first loop, and some improvements to it, was closed and operated. The second loop shown comes closest to having the open loop gain desired (figure 1), but still falls far short of that goal.

#### a. 350 Hertz Mirror Loop

The first attempt at closing the loop, taking into account preliminary actuator characteristics, is shown in the block diagram of figure 16. The load model is the load mass/magnetic spring characteristics with a linear friction damping modeled on the basis of open loop results. The compensation was chosen to provide a phase greater than  $-180$  degrees at low frequencies and considerable phase margin at the 350 Hz calculated crossover. The goal was to provide a loop that was not conditionally stable. Open loop gain and phase plots are shown in figure 17. The open loop gain goal is also shown; this goal is the minimum required for base motion following with the LPS isolated base motion spectrum, shown previously in figure 1. This loop was closed with marginal results. A number of problems were discovered. At the calculated gain settings, the loop had a low amplitude oscillation at 450 to 500 Hz indicating higher gain at the phase crossover. The gain was lowered and a stable loop resulted. Ripple from the position transducer, at 11.5 and 23 KHz, caused a large ripple in the current loops, tending to saturate those loops. The loop was very sensitive to saturation when given a commanded input, with a tendency to limit cycle at large amplitude at 25 to 30 Hz, indicating greater phase shift at low frequency than shown in figure 17. Various other compensation schemes similar to this test were tried with somewhat the same results.

Although some of these schemes had somewhat better results than others, all the compensation loops of this type had open loop gain characteristics considerably below what is required. It was therefore decided to perform tradeoff studies to determine what compensation was potentially feasible which would achieve a gain characteristic near the goal.

#### b. Integrally Compensated Loop

Figure 18 presents a block diagram of the compensated loop that comes closest to achieving the gain goal. No transducer phase lag characteristic is used. The final two filters (at 12560 and 50000 rad/sec) in the compensation

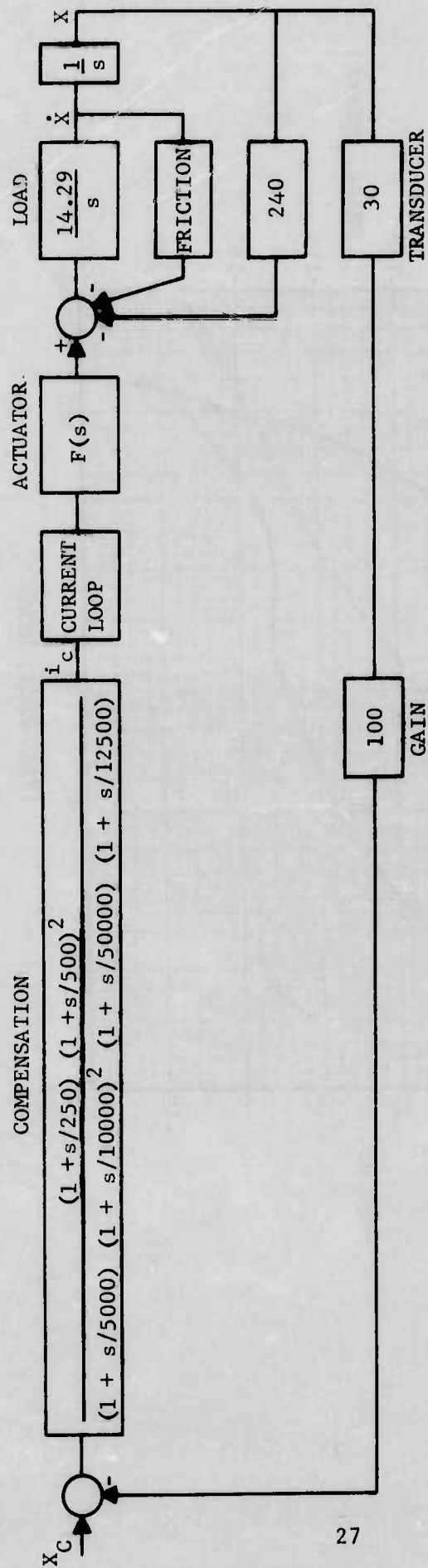


Figure 16. Block Diagram: 350 Hertz Mirror Position Loop



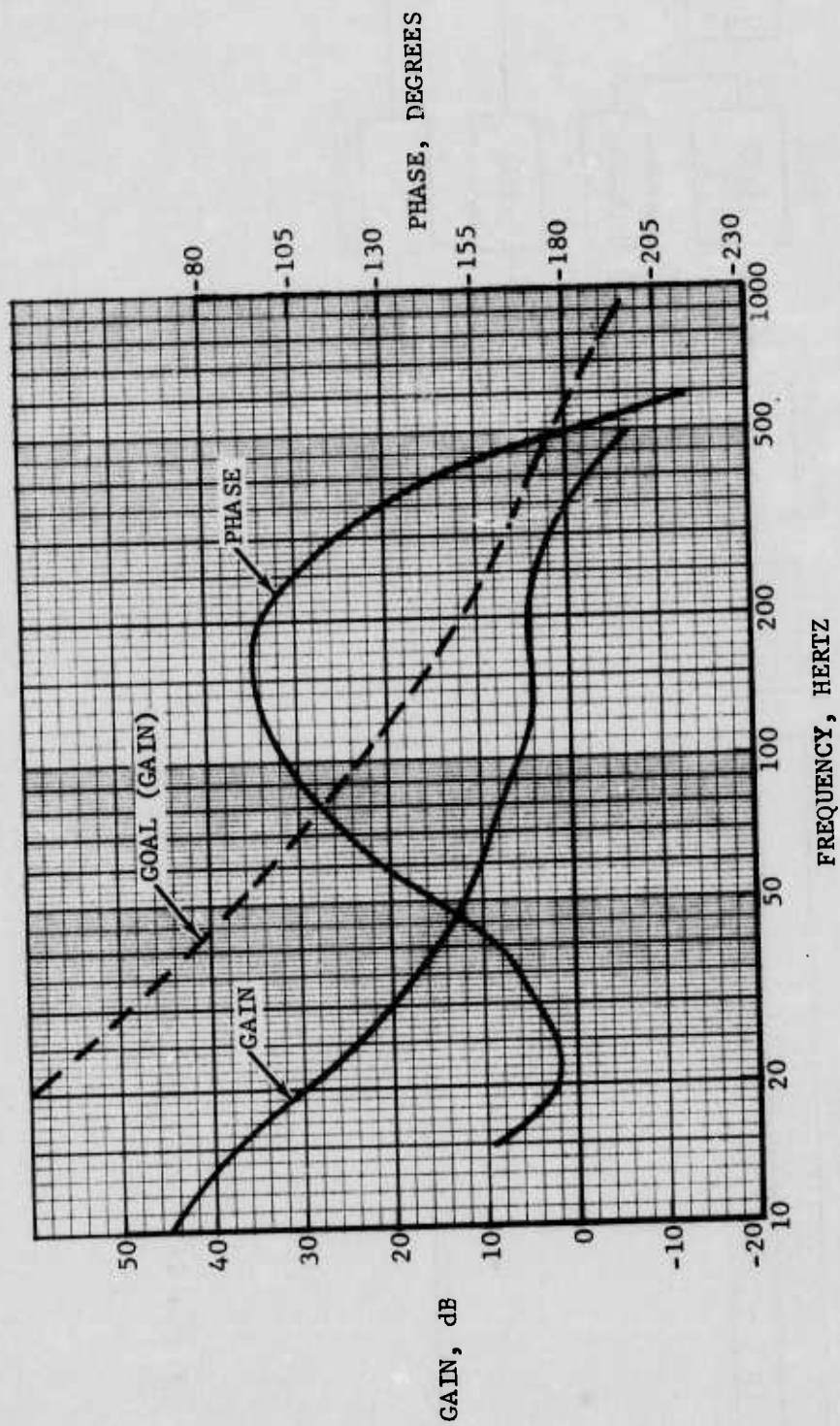


Figure 17. Open Loop Response: 350 Hertz Mirror Position Loop

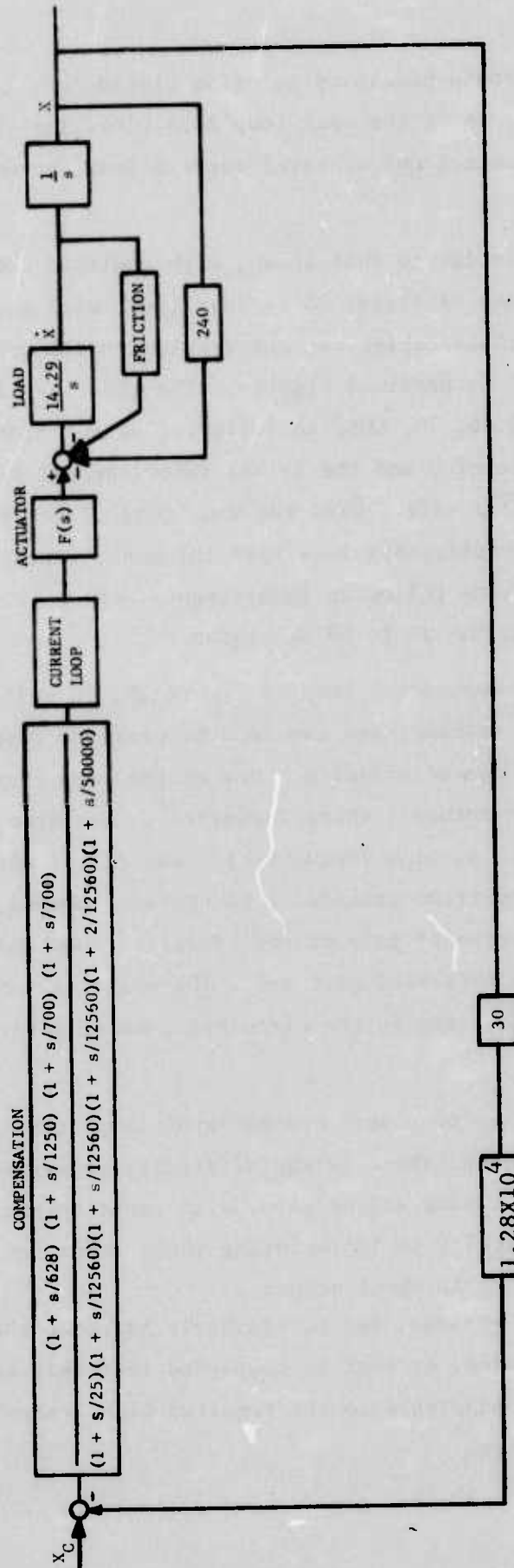


Figure 18. Block Diagram: 300 Hertz Mirror Loop with Integral Compensation

represent filters found necessary in prior closed loop tests to minimize noise effects. Figure 19 shows the open loop Bode plots for this loop, using the theoretical compensation and measured current loop, actuator, and load characteristics.

This loop is similar to that shown, with modified compensation, in figure 20. The control loop of figure 20 is idealized, with perfect actuator and current amplifier characteristics, and results in the open loop gain plot shown as the "goal" in previous figures. The idealized loop results in a relative error of 0.46, 1σ, LOS, in following base motion when used with a system magnification of 5 and the latest autoalignment mirror design with a 2:1 axis and a  $\sqrt{2}$ :1 axis. Thus the two "real" loops shown here, figures 17 and 19, with gain considerably less than the goal, would fall far short of meeting the base motion following requirements, which is particularly sensitive to open loop gain in the 20 to 50 Hz region.

The integrally compensated loop of figure 18, in addition to the integral compensation at 25 rad/sec, has two lead networks to compensate for the actuator gain and phase loss characteristics. One of the more serious drawbacks to compensating for the actuator characteristics as was done in both of these loops is the increased gain at high frequencies. The difference in high frequency compensation, from position transducer to current command, is shown in figure 21. Shown is the high frequency gain of the idealized loop and the two loops presented here. The vastly increased gain makes the position loops with this actuator far more sensitive to noise in the circuitry, and in particular to transducer noise and ripple.

In addition to the "on paper" drawbacks of loops configured with the measured actuator characteristics, there is the difficulty presented by the variation of actuator phase, and to some extent gain, with input current level. This presented considerable difficulty in implementing these loops, and made them quite susceptible to limit cycle oscillations.

For all of these reasons, but particularly based on the actuators loss of gain at high frequencies, it must be concluded that this actuator, in its present form, is not readily adaptable to the required high frequency autoalignment mirror actuation system.

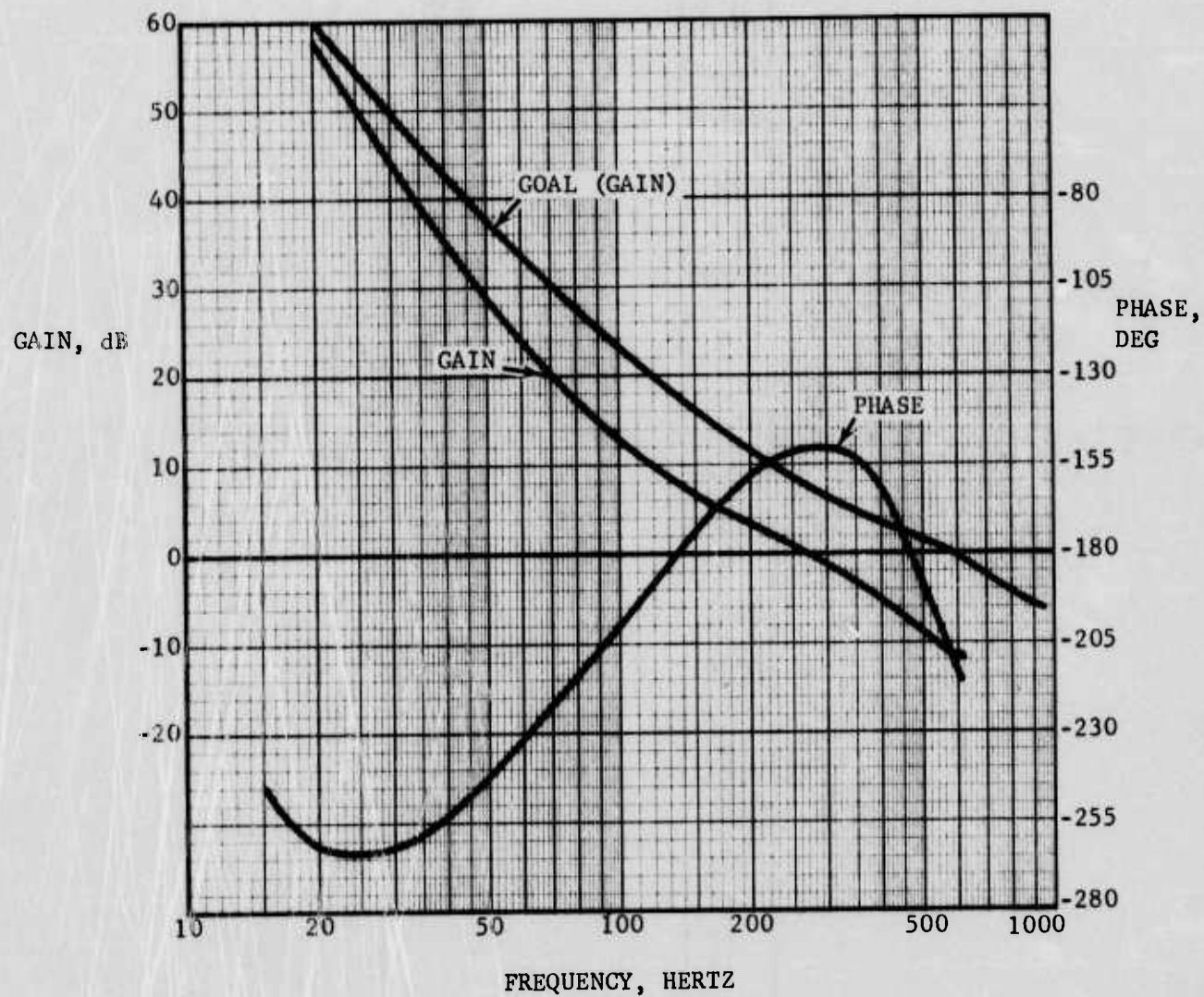


Figure 19. Open Loop Response: 300 Hertz Mirror Loop



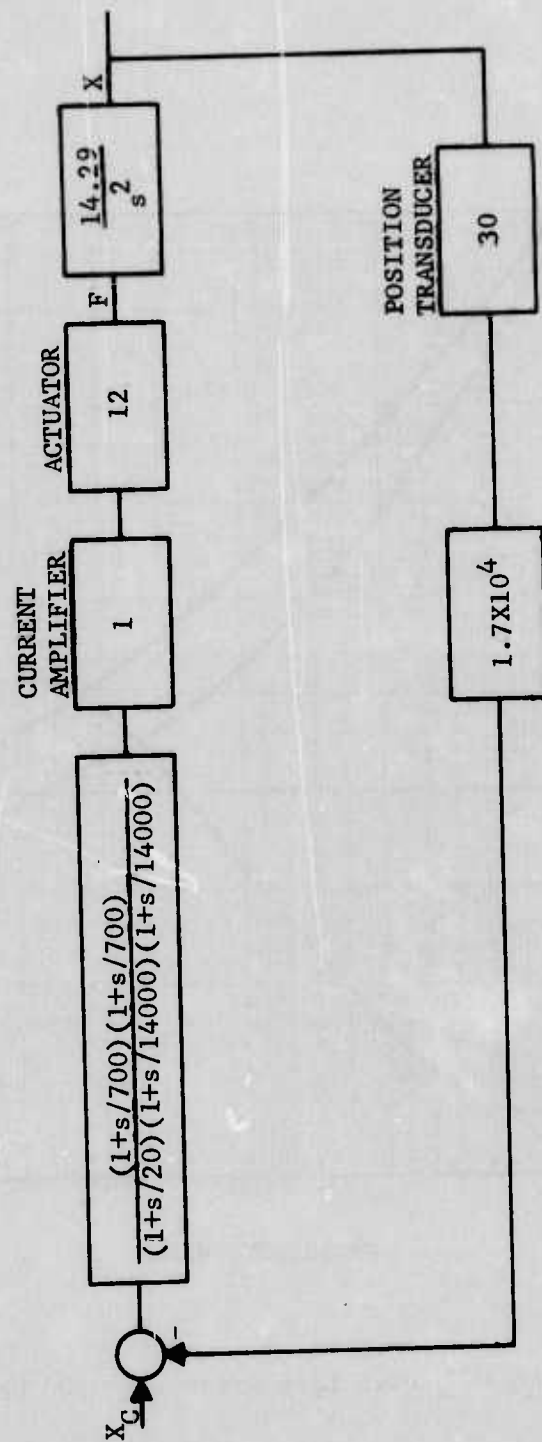


Figure 2C. Idealized Loop Resulting in Open Loop Gain "Goal"

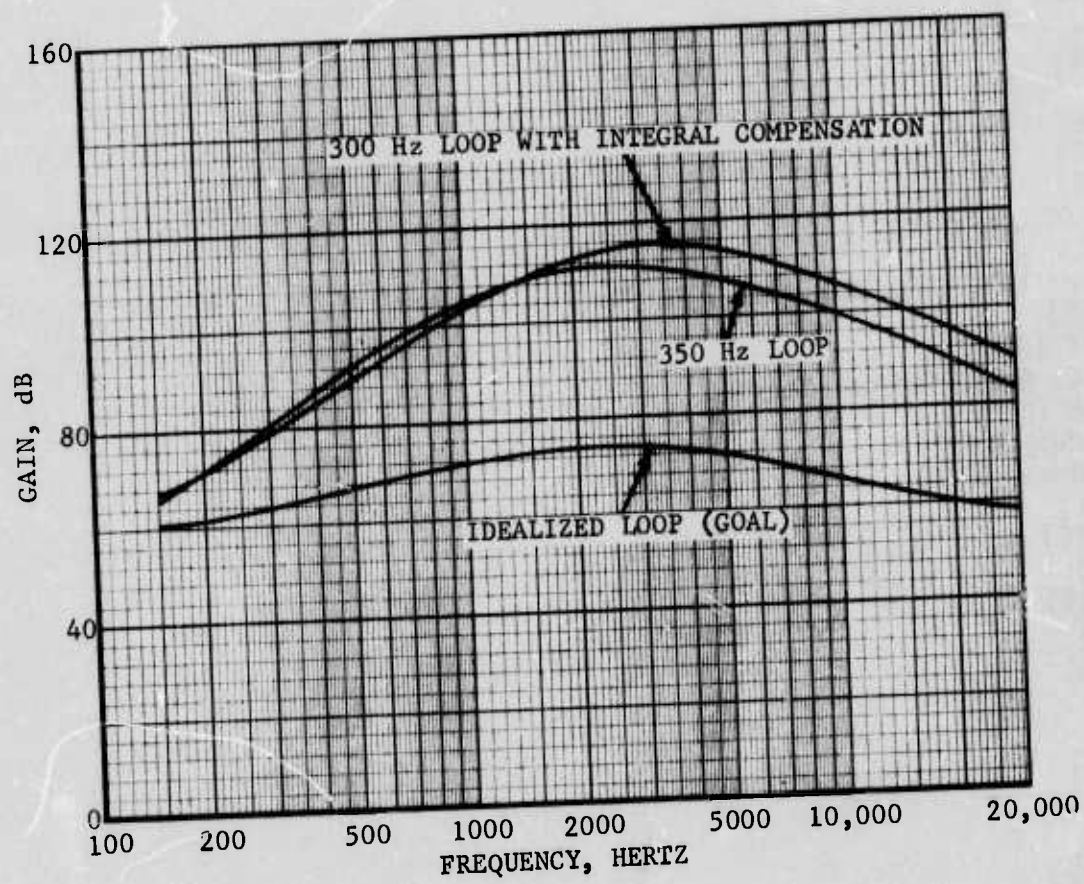


Figure 21. High Frequency Compensation Gain Comparison

# DISTRIBUTION

Hq USAF (SAMI)	1	Fclty Eng Sup Agency (FESA-RTD)	1
Hq USAF (PRE)	1	CERL	1
Hq USAF (PREE)	1	NFEC	1
Hq USAF (PREV)	1	DDC (TCA)	2
Hq USAF (PREPB)	1	Offl Record Cy (Capt Gogosha/LRO)	1
Hq USAF (RDPQ, 1C370)	1		
SAF	1		
AFCEC (PREC)	3		
AFISC (PQAL)	1		
Nuc Safety (SN)	1		
AFSC (DOB)	1		
AFSC (DLCAW)	1		
TAC (DEE)	1		
CINCSAC (DEE)	1		
AFLC (DEE)	1		
ADC (DEE)	1		
AUL (LDE)	1		
AU (ED, Dir, Civ Eng)	1		
AAC (DEE)	1		
AFIT (Tech Lib, Bldg 640, Area B)	1		
AFIT (CES)	1		
CINCUSAFE (DEE)	1		
USAF, SCLO (Maj Pierson) Canada	1		
CINCPACAF (DEE)	1		
USAF Academy (DFS LB)	1		
USAF Academy (DFCE)	1		
5 AF (DEE)	1		
13 AF (DEE)	1		
ASD (DEE)	1		
SAMSO (DEE)	1		
ESD (DEE)	1		
RADC (DEE)	1		
AFWL (HO)	1		
AFWL (DE)	1		
AFWL (DEE)	1		
AFWL (DEZ)	15		
AFWL (WE)	1		
AFWL (SUL)	2		
AFOSR	1		
AWS (AWVAS)	1		
TAC (DEE)	1		
Reg Civ Eng GA	1		
Reg Civ Eng, CA	1		
Reg Civ Eng, TX	1		
Chief of Eng (DAEN-RDM)	1		
Eng WW Exp Sta (WESSS)	1		
ONR (Code 418)	1		
NWC (Code 753)	1		
OIC, USNCB Center	1		
NCEL	1		
11 WS/DON	1		
FTD/WE	2		

**THIS REPORT HAS BEEN DELIMITED  
AND CLEARED FOR PUBLIC RELEASE  
UNDER DOD DIRECTIVE 5200.20 AND  
NO RESTRICTIONS ARE IMPOSED UPON  
ITS USE AND DISCLOSURE.**

**DISTRIBUTION STATEMENT A**

**APPROVED FOR PUBLIC RELEASE,  
DISTRIBUTION UNLIMITED.**